Modeling Earth Systems and Environment (2020) 6:1201–1221
https://doi.org/10.1007/s40808-020-00751-8

ORIGINAL ARTICLE

The 2000–2017 drought risk assessment of the western and southwestern basins in Iran

Iman Rousta[1,2] · Haraldur Olafsson[3] · Md Moniruzzaman[4] · Jonas Ardö[5] · Hao Zhang[6] · Terence Darlington Mushore[7] · Shifa Shahin[8] · Saiful Azim[9]

Received: 25 January 2020 / Accepted: 17 March 2020 / Published online: 27 March 2020

Abstract

The study investigates the relationship between drought and vegetation variations in three main basins of western and southwestern of Iran, using the comprehensive approach of time-series analysis, Standardized Precipitation Index (SPI), and anomaly calculation. A total of 30 ground stations' daily meteorological data and the MODIS 16-day composite NDVI products (2000–2017) were used in this case. The results showed that in the Great Karoun River (GKRW) and Karkheh River (KRW) sub-regions, the NDVI decreased slightly over the study period. Simultaneously, in the West Marginal (WMW) sub-region the NDVI slightly increased somewhat. Overall, the NDVI in the whole study area presented an insignificant decrease. Also the results found that there is a significant relationship ($p < 0.02$) between the NDVI (0.3–0.7) with spring drought and between NDVI (0.2–0.3) with fall drought ($p < 0.01$). There is a marginally significant relationship ($R = 0.43$, $p = 0.07$) between NDVI (0.3–0.4) with fall drought and a relatively high, but insignificant relationship between NDVI (0.7–0.8) with spring drought ($R = 0.41$, $p = 0.09$). Low temperature can play an important role in determining the relationship between SPI and NDVI, which evidenced that it can trade-off the effect of a very wet year. As well as a year with very wet condition can affect the NDVI of the coming years. Since summer is hot season in the study area and most of the vegetation consists of shrubs and grasslands, of which the NDVI ranges between 0.2 and 0.4, the vegetation cover can be significantly affected by a wet summer with abundant precipitation.

Keywords Vegetation · Drought · Precipitation · Temperature · NDVI · SPI · Time series

✉ Iman Rousta
irousta@yazd.ac.ir

✉ Hao Zhang
zhokzhok@163.com

Haraldur Olafsson
haraldur68@gmail.com

Md Moniruzzaman
moniruzzaman1313ku@gmail.com

Jonas Ardö
jonas.ardo@nateko.lu.se

Terence Darlington Mushore
tdmushore@science.uz.ac.zw

Shifa Shahin
shifashahin786@gmail.com

Saiful Azim
saz@plen.ku.dk

[1] Department of Geography, Yazd University, Yazd 8915818411, Iran

[2] Institute for Atmospheric Sciences-Weather and Climate, University of Iceland and Icelandic Meteorological Office (IMO), Bustadavegur 7, IS-108 Reykjavik, Iceland

[3] Institute for Atmospheric Sciences-Weather and Climate and Department of Physics, University of Iceland, and Icelandic Meteorological Office (IMO), Bustadavegur 7, IS-108 Reykjavik, Iceland

[4] Center for Space Science and Technology in Asia and the Pacific (CSSTEAP), Dehradun 248001, India

[5] Department of Physical Geography and Ecosystem Science, Lund University, Sölvegatan 12, 223 62 Lund, Sweden

[6] Department of Environmental Science and Engineering Jiangwan Campus, Fudan University, 2005 Songhu Road, Yangpu District, Shanghai 200438, China

[7] Department of Physics, Faculty of Science, University of Zimbabwe, MP167 Mt Pleasant, Harare, Zimbabwe

[8] Department of Agriculture and Food Engineering, Indian Institute of Technology (IIT), Kharagpur, India

[9] Department of Plant and Environmental Science, University of Copenhagen, Copenhagen, Denmark

Introduction

Drought is a common natural disaster and hostile climatic phenomenon which requires detection and monitoring of water stress to manage it. It has significant adverse impacts on human life (agricultural, environmental, hydrological and socio-economic), wildlife and plant communities (Bhuiyan et al. 2006; Goddard et al. 2003; Khosravi et al. 2017; Rahimzadeh-Bajgiran et al. 2012). Semiarid regions which include 61% of Iran are characterized by low and varying yearly precipitation (Rahimzadeh-Bajgiran et al. 2012; Rousta et al. 2014, 2017a, b, c, 2018a; 2020). As a result, vegetation and soil water stress have become a major widespread problem in semiarid countries such as Iran. Vegetation condition monitoring offers great potential for detection of droughts toward alleviation of its adverse socio-economic impacts.

There has been increasing studies on various indices and methods for drought study using diverse drought-causative and drought-responsive parameters (Gibbs 1967; Kogan 1990, 2002; McKee et al. 1993; Palmer 1965, 1968; Shafer 1982). The frequently used parameters include precipitation, soil moisture, effective evapotranspiration, vegetation dynamics, and ground- and surface-water conditions. All of these are not linearly linked to one another but often found a weak correlation between themselves. It has become a common phenomenon that different drought indices identify a particular place contrarily at the same time (Bhuiyan 2004). Therefore, drought perception varies significantly among different climatic regions (Dracup et al. 1980). This makes area-specific evaluation of indices to determine their effectiveness in quantifying drought conditions important.

Agricultural and vegetative drought can be used as an indicator of meteorological and hydrological droughts. In consequence, soil moisture, streamflow, reservoir storage, and groundwater level reflect drought impacts in the condition of precipitation deficiency. On the basis of meteorological data, several climatic and hydrological drought indices (point-based) have been found. The major challenge with in situ datasets is that they are often insufficient, poorly distributed and not available for timely water stress and drought detection. Alternatively, the remote sensing technique enables monitoring of water stress at higher temporal or spatial resolutions in an economical way with lower cost and time. Numerous satellite-retrieved indices have been established since the 1980s to investigate vegetation condition and soil moisture for drought monitoring (Rahimzadeh-Bajgiran et al. 2012). For instance, the NOAA-operated advanced very-high-resolution radiometer (AVHRR) data were the first remotely sensed data used for monitoring vegetation condition and changes with the normalized difference vegetation index (NDVI). Over the years, other datasets such as MeteoSat, MODIS and Landsat series were used for similar purposes at a variety of temporal and spatial scales. Due to ease of access and huge records of archival data, most of these datasets can be used in different areas to improve monitoring and modeling of droughts.

Retrieval of drought indices such as Standardized Precipitation and Evaporation Index (SPEI) and Standardized Precipitation Index (SPI) has been done using both remotely sensed and in situ data. For instance, Bordi and Sutera (2001, 2002) studied the large-scale analysis of drought variability by assessing drought occurrence by means of the Standardized Precipitation Index (SPI) developed by McKee et al. (1993) and the Palmer Drought Severity Index (PDSI) developed by Palmer (1965). The SPI has several characteristics that are an upgrade over other indices, with its simplicity and flexibility. The PDI has a complex structure than SPI (Guttman 1998). In the deserts of Northern America, Ji and Peters (2003) performed a study on vegetation (grass vegetation and farming lands) response to accessible humidity by investigating SPI and NDVI indices. Based on three fundamental methods, i.e., SPI and NDVI indices in various time scales (1, 2, 3, 6, 9, and 12 months), they obtained that three months was the best cohesion between NDVI and SPI. In the same study, the best relation between SPI and NVDI was found in regions with low soil water-storing capacity (Ji and Peters 2003).

In Aravalli, India, drought dynamism was monitored by Bhuiyan et al. (2006) using meteorological and satellite-derived indices from 1984 to 2003. They employed the SPI index to determine the rainfall deficit and the Standardized Water Level Index for evaluating shortcoming and drainage of underground water. Also, computed NOAA AVHRR thermal channel data and Global Vegetation Index (GVI) derived Temperature Condition Index (TCI), Vegetation Health Index (VHI) and Vegetation Condition Index (VCI) for monsoon and non-monsoon seasons drought analysis. They have found that negative SPI anomalies do not always correspond to drought. They also observed that aquifer-stress shifts its position with respect to time in the study area (Bhuiyan et al. 2006). Bajgiran et al. (2008) studied the possibilities of drought monitoring using NDVI and vegetation cover indices (VCI) derived from AVHRR, NOAA in the northwest of Iran. They found the best cohesion between NDVI and VCI by 3-monthly rainfall, and compared with VCI, also achieved a better conformity between the NDVI and the rainfall. Evidently, vegetation conditions relate to drought severity with extents of correlation varying from place to place (Bajgiran et al. 2008). Establishment of area-specific association between the vegetation indices and droughts is thus important.

Table 1 Description of study area watersheds

Watershed	Area (km^2)	Average elevation (m)	Yearly average precipitation (mm)
Western Marginal	35,058	968	499
Karkheh River	51,643	1055	399
Great Karoun River	67,257	1226	448

In the sense of ecological sustainability, Iran is subject to the deforestation, desertification, and severe soil erosion. Iran's most of the watershed areas and their critical points are located in mountainous and hilly areas. All these areas usually have thinly scattered masses or no tree cover. On the other hand, the Iranian watersheds are the most important basins in terms of agriculture and flood management. Studying vegetation dynamics and their link to drought in these basins is very important to the ecological sustainability of the country. The objective of this study is thus to investigate the cause–effect relationship between vegetation and drought stress as well as their strengths via remotely sensed vegetation and drought indices in the Iranian watersheds.

Materials and methods

Study area

The study area is located in the west and southwest of Iran (in between latitudes of 30° 2′ to 35° 8′ N and 45° 39′ to 52° 02′ E longitude), covering three main watersheds (approximately 149,000 km^2) known as Western Marginal (WM), Karkheh River (KRW) and Great Karoun River (GKRW) watersheds (Table 1 and Fig. 1). The WM is located on the western border of Iran and bordered by Iraq, and this basin is the first region of the Persian Gulf catchment area. The area of the basin is 35,058 km^2, of which 81% is mountains, and the rest are plains, foothills and valleys. The 50-year average rainfall of the basin is 455 mm. The KRW is one of the second-order basins of the Persian Gulf and one of the six first-order or major basins of Iran. The basin is located in southwest of Iran with elongated tributaries to the central part of the country. It originates from high mountains in the northwest of Iran and terminates at Hour-Al Azim on the Iran–Iraq southern border. The Karkheh highlands and rugged terrain on the upper part receive considerable precipitation as rain or snow in the mountainous parts, where the river tributaries originate with permanent streams that eventually join to form the Karkheh River. Water scarcity is a dominant problem in KRW dry areas. The highest point elevation of the KRW is 3645 m above mean sea level. The KRW extends over 51,643 km^2, which is 3.2% of Iran, and has a perimeter of 1891 km of which 55.5% is in mountainous regions, and 44.5% are in foothills and plains. The climate of the Karkheh River is dry and semiarid with mild and humid winters and hot and dry summers. The 50-year average rainfall of the basin is 417 mm. The Great Karun River has a length of 890 km, 67,257 km^2 area, 0.3% average slope, 18,700 million km^3 average annual discharge, and 626-mm 50-year average rainfall is considered to be the most watery and longest river in Iran. Of this basin, 67% is in mountainous and foothill regions and 33% in high plains.

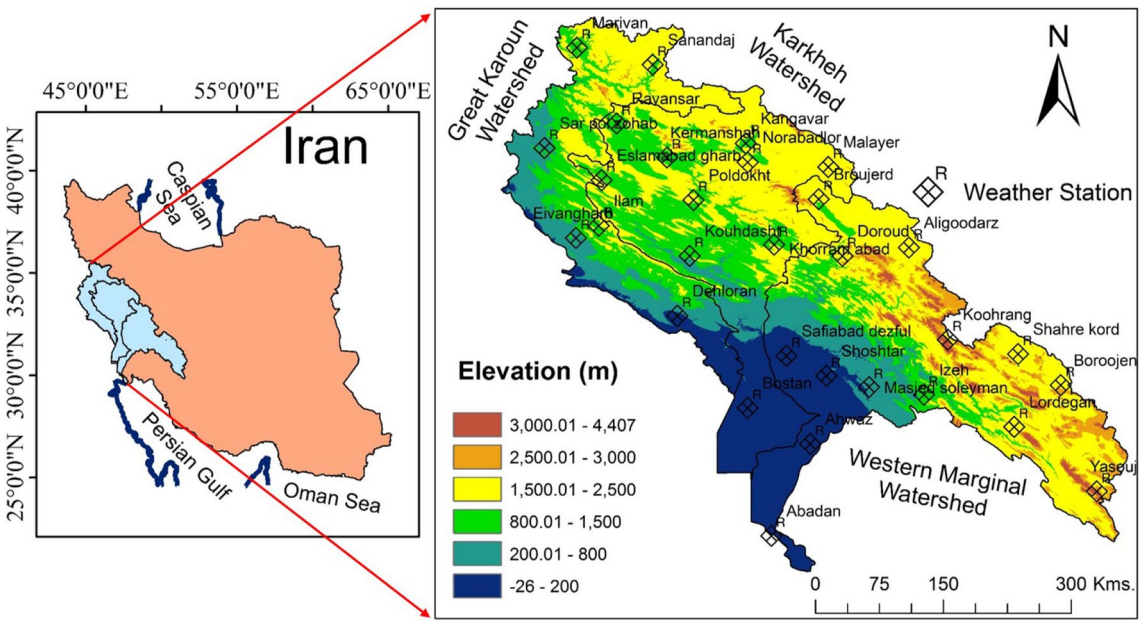

Fig. 1 Study area showing elevation and 30 weather stations

This basin is the third region of the Persian Gulf catchment area (Table 1 and Fig. 1). Winter and spring seasons are special seasons in the study area, because this is the wettest period. So, these seasons have the potential to significantly affect the annual mean SPI.

Methodology

To monitor the intensity, duration, and spatial extent of drought, daily precipitation data recorded at 30 stations (Fig. 1 and Table 10) in 2000–2017 were obtained from IRIMO.[1] Precipitation data quality was controlled using the Gamma distribution technique. Many studies have employed the gamma distribution in the analysis of rainfall (Fernandez-Raga et al. 2017; Smitha et al. 2018; Yu et al. 2017).

Precipitation data over the area of study were used to compute the 4- and 12-month SPI. In order to monitor vegetation variations in space and time, NDVI derived from MODIS satellite data was used. The images were retrieved by using Application for Extracting and Exploring Analysis Ready Samples (AρρEEARS) software from https://lpdaacsvc.cr.usgs.gov.appeears (Didan 2015). MODIS products that were used for this research included MOD13Q1.006 at 250-m spatial resolution, and its composite period is 16 days for a study period from February 2000 to December 2017. The study used a total of 411 images covering whole the study area, and spatial analysis was performed using ESRI ArcGIS 10.7. Details on retrieval of drought and vegetation indices are provided in following sections.

Normalized difference vegetation index (NDVI)

NDVI index is useful for estimation of biomass potential, which is measured with leaf area index (LAI) and production pattern (Dutta et al. 2015; Gitelson et al. 2003; Tarpley et al. 1984; Thenkabail and Gamage 2004). Over the recent years, NDVI has been used by many scientists in different studies based on vegetation classification, land-use/land-cover changes, vegetation phenology, mapping of continental land cover, and vegetation dynamics (Geerken et al. 2005; Martínez and Gilabert 2009; Moulin et al. 1997; Mushore et al. 2019; Rousta et al. 2018b; Running et al. 1995; Townshend and Justice 1986). NDVI is one of the suitable indices for monitoring drought, estimating healthy status of vegetation, crop growth conditions and crop yields (Dabrowska-Zielinska et al. 2002; Dutta et al. 2015). The basic concept of NDVI is the fact that internal mesophyll structure of healthy green leaves highly reflects near-infrared (NIR) radiation, whereas the leaf chlorophyll and other pigments absorb a large proportion of the red visible (VIS) radiation. This function of internal leaf structure becomes reversed in case of unhealthy or water stressed vegetation (Chanklan et al. 2017; Dutta et al. 2015; Ghafarian Malamiri et al. 2018). NDVI is calculated by the difference between reflectance in near-infrared (NIR) and visible red (VIS) band of electromagnetic spectrum (Eq. 1)

$$\mathrm{NDVI} = \frac{\mathrm{NIR} - \mathrm{VIS}}{\mathrm{NIR} + \mathrm{VIS}} \tag{1}$$

The value of NDVI ranges between −1 and +1. Very low value of NDVI (≤ 0.1) corresponds to snow, sand or rocky bare areas. Moderate NDVI values from 0.2 to 0.3 represent shrub and grassland, while high NDVI values (0.6–0.8) indicate tropical and temperate rainforests. NDVI values which are closest to 0 represent bare, while negative NDVI values correspond water bodies (Gandhi et al. 2015).

Based on the MODIS 16-day NDVI images with 250-m resolution, for the whole study area and three watersheds, seasonal and annual NDVIs as well as inter-annual anomaly of NDVI were calculated As well as we have calculated the coverage for each of the NDVI classes for the whole study area and also for each watershed separately. Spatial extents of seasonal and annual NDVIs with eight categories (0.2–0.3, 0.3–0.4, 0.4–0.5, 0.5–0.6, 0.6–0.7, 0.7–0.8, 0.8–0.9, and 0.9–1) were generated with ArcGIS 10.7.

Calculation of NDVI anomaly

The seasonal and annual anomalies rates of the NDVI were calculated for each pixel in the study area and during 2000–2017. Anomalies are calculated using Eq. 2 and Eq. 3 below:

$$\mathrm{NDVI_{YA}} = (\mathrm{NDVI}_{xi} - \mathrm{NDVI}_{\bar{x}})/\delta \rightarrow \left\{ \begin{array}{l} > 0 \,\text{Positive Anomaly} \\ < 0 \,\text{Negative Anomaly} \end{array} \right\} \tag{2}$$

$$\mathrm{NDVI_{SA}} = (\mathrm{NDVI}_{xi} - \mathrm{NDVI}_{\bar{x}})/\delta \rightarrow \left\{ \begin{array}{l} > 0 \,\text{Positive Anomaly} \\ < 0 \,\text{Negative Anomaly} \end{array} \right\} \tag{3}$$

where $\mathrm{NDVI_{SA}}$ and $\mathrm{NDVI_{YA}}$ are seasonal (SA) and yearly (YA) anomalies of NDVI for each pixel, respectively, NDVI_{xi} is the average of seasonal and yearly NDVI for each year, and $\mathrm{NDVI}_{\bar{x}}$ is the average of seasonal and yearly NDVI for whole study period in 2000–2017, and δ is the standard deviation.

Standardized Precipitation Index (SPI)

To monitor drought, McKee et al. (1993) had developed the Standardized Precipitation Index (SPI). And to fit climatological precipitation time series, Thom (1966a) found the

[1] Islamic Republic of Iran Meteorological Organization.

Table 2 Wet and drought period classification according to the SPI index (Cancelliere et al. 2007; Shah et al. 2015)

Index value	Class	Description	Probability	Δp
Non-drought	SPI ≥ 2.00	Extremely wet	0.977–1.000	0.023
	1.50 ≤ SPI < 2.00	Very wet	0.933–0.977	0.044
	1.00 ≤ SPI < 1.50	Moderately wet	0.841–0.933	0.092
	−1.00 ≤ SPI < 1.00	Near normal	0.159–0.841	0.682
	−1.50 ≤ SPI < − 1.00	Moderate drought	0.067–0.159	0.092
	−2.00 ≤ SPI < − 1.50	Severe drought	0.023–0.067	0.044
	SPI < − 2.00	Extreme drought	0.000–0.023	0.023

Table 3 Wet and drought period classification used in this study

Index value	Class	Description	Probability	Δp
Non-drought	SPI ≥ 2.00	Extremely wet	0.977–1.000	0.023
	1.50 ≤ SPI < 2.00	Very wet	0.933–0.977	0.044
	1.00 ≤ SPI < 1.50	Moderately wet	0.841–0.933	0.092
	0.00 ≤ SPI < 1.00	Slight wet (near normal)	0.159–0.841	0.341
	−1.00 ≤ SPI < 0.00	Slight drought (near normal)	0.159–0.841	0.341
	−1.50 ≤ SPI < − 1.00	Moderate drought	0.067–0.159	0.092
	−2.00 ≤ SPI < − 1.50	Severe drought	0.023–0.067	0.044
	SPI < − 2.00	Extreme drought	0.000–0.023	0.023

gamma distribution, which is outlined by its frequency or chance density function (McKee et al. 1993; Thom 1966b):

$$f(x) = \frac{1}{\beta^{\alpha}\tau^{\alpha}} x^{\beta-1} e^{-x/\beta} \tag{4}$$

where $\alpha > 0$, α is a shape factor, $\beta > 0$, β is a scale factor, x is equal to all nonzero values in the precipitation history. It is assumed that $\alpha > 0$ and $\beta > 0$. The gamma function may be expressed as follows:

$$\Gamma(\alpha) = \int_0^{\infty} e^{-t} t^{\alpha-1} \mathrm{d}t \tag{5}$$

where $\Gamma(\alpha)$ is the gamma function.

Fitting a gamma probability density function to a given frequency distribution of overall precipitation for a station is done as part of computation of the SPI. From Thom (1966a, b), the maximum likelihood solutions are used to optimally estimate α and β

$$\dot{\alpha} = \frac{1}{4A}\left(1 + \sqrt{1 + \frac{4A}{3}}\right) \tag{6}$$

$$\dot{\beta} = \frac{\bar{x}}{\alpha} \tag{7}$$

$$A = \ln \bar{x} - \frac{\sum \ln(x)}{n} \tag{8}$$

where n = number of precipitation observations, A is a measure of the skewness of the distribution, $\bar{x}$ is the arithmetic mean of all nonzero values.

The cumulative probability is given by:

$$G(x) = \int_0^x g(x)\mathrm{d}x = \frac{1}{\dot{\beta}^{\dot{\alpha}}\tau^{\dot{\alpha}}} \int_0^x x^{a-1} e^{-x/\beta} \tag{9}$$

Letting, $t = x/\beta$

$$G(x) = \frac{1}{\Gamma \dot{a}} \int_0^x t^{a-1} e^{-t} \mathrm{d}t \tag{10}$$

The gamma function is undefined for $x = 0$, and a precipitation distribution may contain zeros, the cumulative probability becomes

$$H(x) = q + (1 - q)\, G(x) \tag{11}$$

where q is the probability of a zero. If m is the number of zeros in a precipitation time series, Thom (1966a, b) states that q can be estimated by m/n. The cumulative probability, $H(x)$, is then transformed to the standard normal random variable Z with mean zero and variance of one, which is the value of the SPI. SPI is categorized based on the range of values shown in Tables 2 and 3. To further evaluate the impact of annual drought on NDVI, the correlation between seasonal coverage of different categories of NDVI values and SPI was calculated for the entire study area.

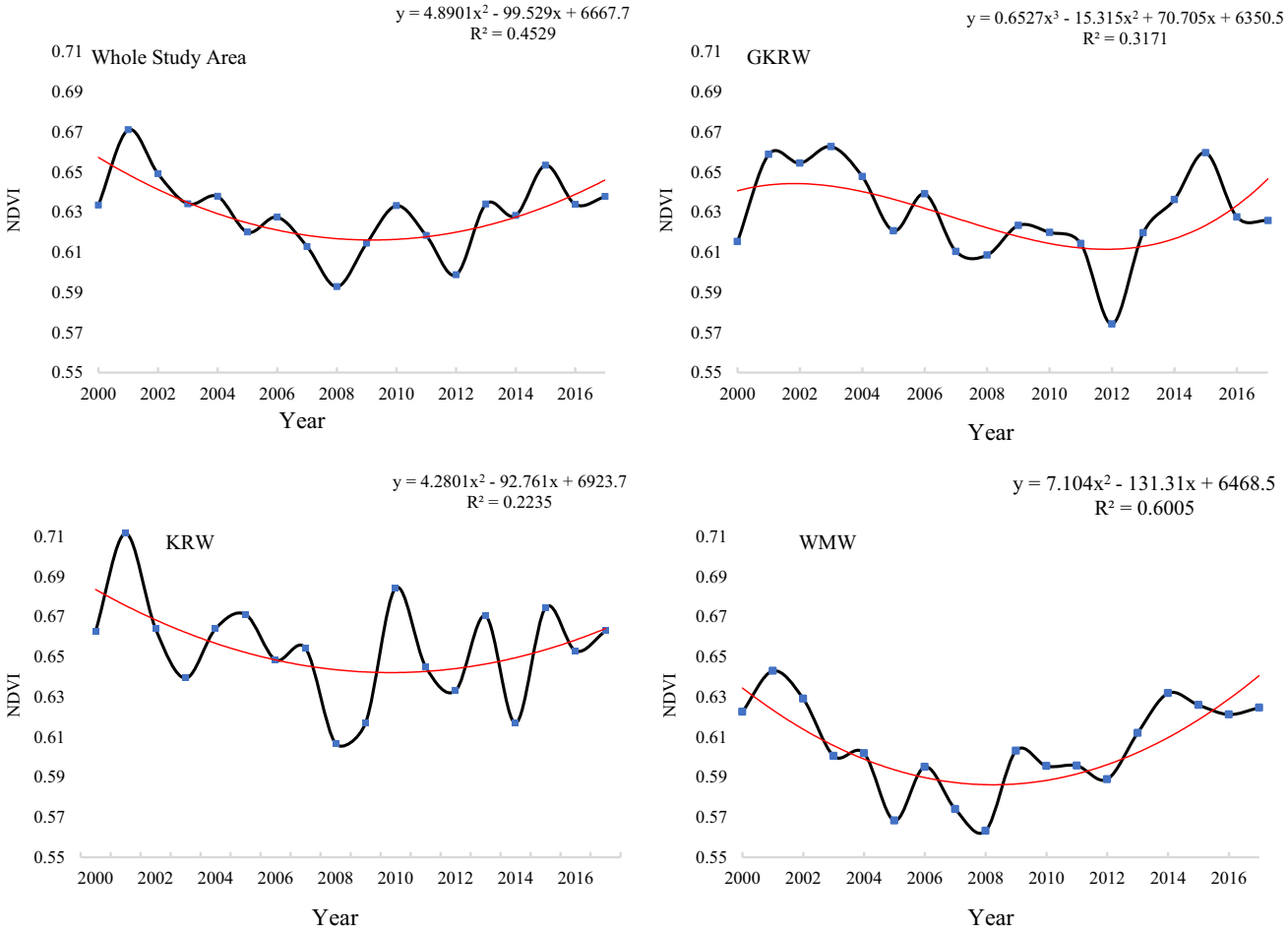

Fig. 2 Time series of average NDVI for the study area and its sub-regions

Results and discussion

NDVI change

The annual variation rates of the NDVI were calculated using the annual mean maximum NDVI of each pixel for the study area and different watersheds during 2000–2017. The temporal trend of annual NDVI showed heterogeneity in the study area, where two regions found slightly decreased NDVI trend and one region showed slightly increased NDVI. Figure 2 shows the temporal trends of the annual max NDVI in the area and its sub-regions. It is clear that there is a slightly decrease rate of average annual NDVI when averaged for the whole study area. The NDVI in the GKRW and KRW sub-regions slightly decreased, and in the WMW sub-region there is a very weak increase in the study period that none of them were statistically significant (Fig. 2).

Spatial patterns of NDVI and SPI trends

Annual mean NDVI showed a slightly decrease trend in the entire study area. Spatial pattern of change trends in seasonal NDVI of some years matched quite well with SPI, for example the year of 2008 was the driest year (SPI − 2. 2) and total area that was covered with vegetation was 14,713 km^2 and also the year of 2015 had the highest value of SPI (2.22), and the vegetation coverage was 25,770 km^2 (Table 2 and Figs. 3, 4, 5). But in some other years such as in 2009 with SPI as 1.61 and vegetation coverage of 21,644 km^2 and year 2017 with SPI − 0.23 and vegetation cover 22,036 km^2, it seems that the harmony has not been cleared. In these cases, it is necessary to check the seasonal SPI and vegetation cover. In the year of 2017, there was a winter with moderate drought (SPI − 1.39) and spring season with moderately wet condition (SPI 1.299), a summer with slight wet condition (0.72 SPI index), and a fall season with slight drought

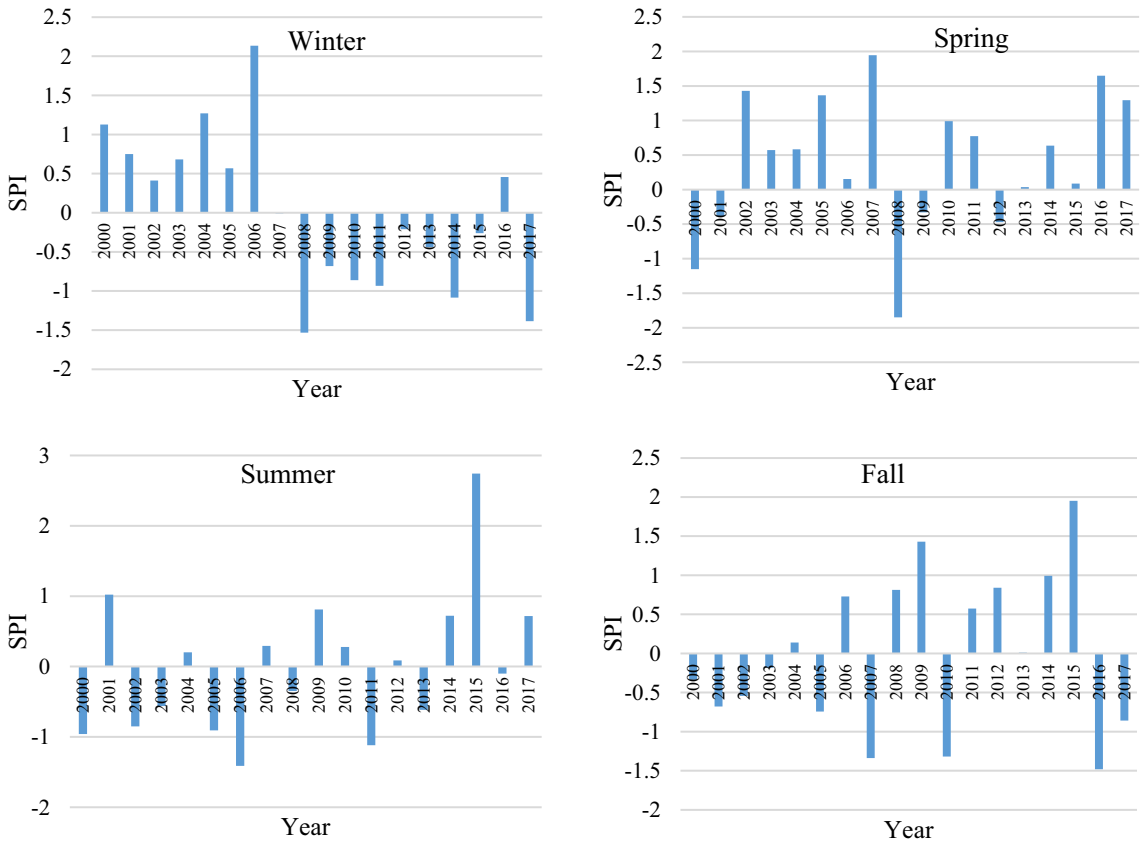

Fig. 3 Seasonal SPI index for whole study area in the period of 2000–2017

condition (−0.86 SPI index). In the year of 2009, there was a winter and spring season with slight drought conditions (−0.68 and −0.33 SPI index, respectively), a summer with slightly wet condition (0.81 SPI index), and a fall season with moderately wet conditions (1.43 SPI index). Overall, it seems that in the study period each year that experienced wetness in winter and spring season, respectively, with SPI index above 0, the coverage of NDVI in that year was near or above the historical average of NDVI of the whole study period (21,404 km^2), and in these cases the role of spring SPI index is more important (Table 4 and Figs. 3, 4, 5). But in some cases as year 2006, other parameters such as temperature can have a significant role, which is interpreted in the next sections.

Table 5 shows the area under each NDVI category in km^2. It is clear that the most common category of NDVI in the study area is 0.2–0.3 that covers about 68% of the vegetation of the study area. The other categories, respectively, include 22.4, 7, 2 and 0.6% of the vegetation of the study area (Table 3). The correlation between different categories of NDVI with yearly SPI showed that there is just a statistically significant correlation between NDVI 0.2–0.3 with yearly SPI ($R=0.50$, $p=0.04$). Also, the correlation between NDVI 0.3–0.4 is relatively high, but it is not statistically significant ($R=0.34$, $p=0.16$). Overall, it seems that most of the vegetation of the study area is shrubs and grasslands and that this kind of vegetation has had a high sensitivity to seasonal SPI (Tables 5, 6).

Drought effects on vegetation productivity at seasonal timescales

The relationship between SPI and spatial coverage of NDVI varied by different NDVI classes (0.2–0.3, 0.3–0.4, 0.4–0.5, 0.5–0.6, 0.6–0.7, 0.7–0.8 NDVI), seasonal variation and by regions. For example, in the study area, spring SPI was significantly correlated with spatial coverage of spring NDVI (0.3–0.7) ($p<0.05$), but the correlation between the NDVI (0.2–0.3) and the NDVI (0.7–0.8) spatial coverage was not statistically significant. Overall, the correlation between SPI

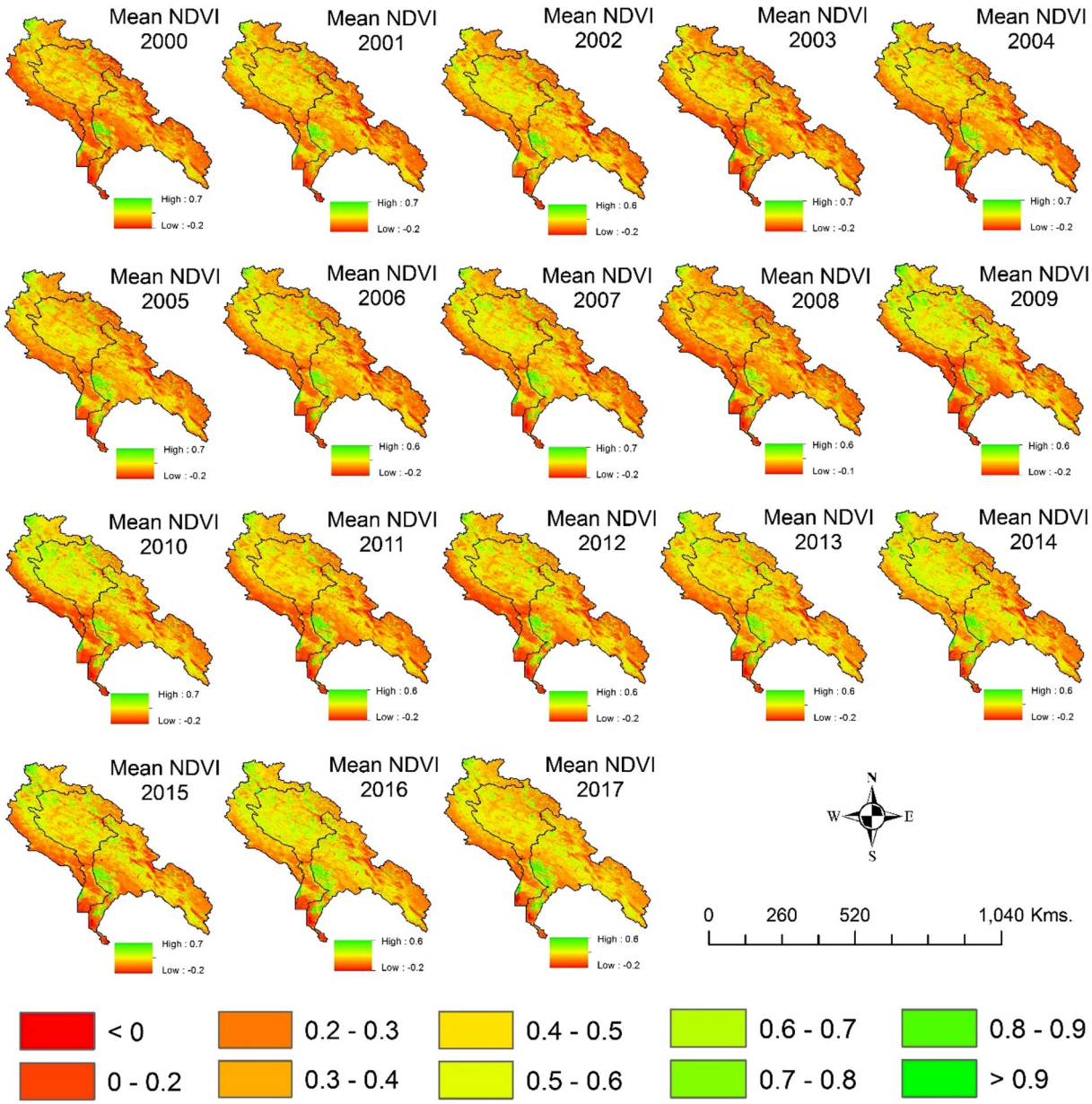

Fig. 4 Annual mean NDVI for the study area during 2000–2017

and spatial coverage of NDVI in the study period for spring and fall seasons was higher than for other seasons (summer and winter) (Table 7).

Winter season is the rainiest and coldest season with average precipitation equal to 213.6 mm and average temperature as 6.2 °C, spring is semi-rainy with moderate temperature (139.1 mm precipitation, 17.1 °C temperature), summer is the driest and hottest season (2.2 mm precipitation and 30 °C temperature), and fall is semi-rainy with cold temperature (88.3 mm precipitation and 19.1 °C temperature). Minimum temperature in all seasons of the study period occurred in Kouhrang station, as well as three of the wettest seasons were observed in this station and the wettest station in summer season in the study area was Malayer station with an average of 8.9 mm precipitation (Fig. 6 and Table 8). So it shows that the winter and spring seasons can significantly affect the annual mean SPI.

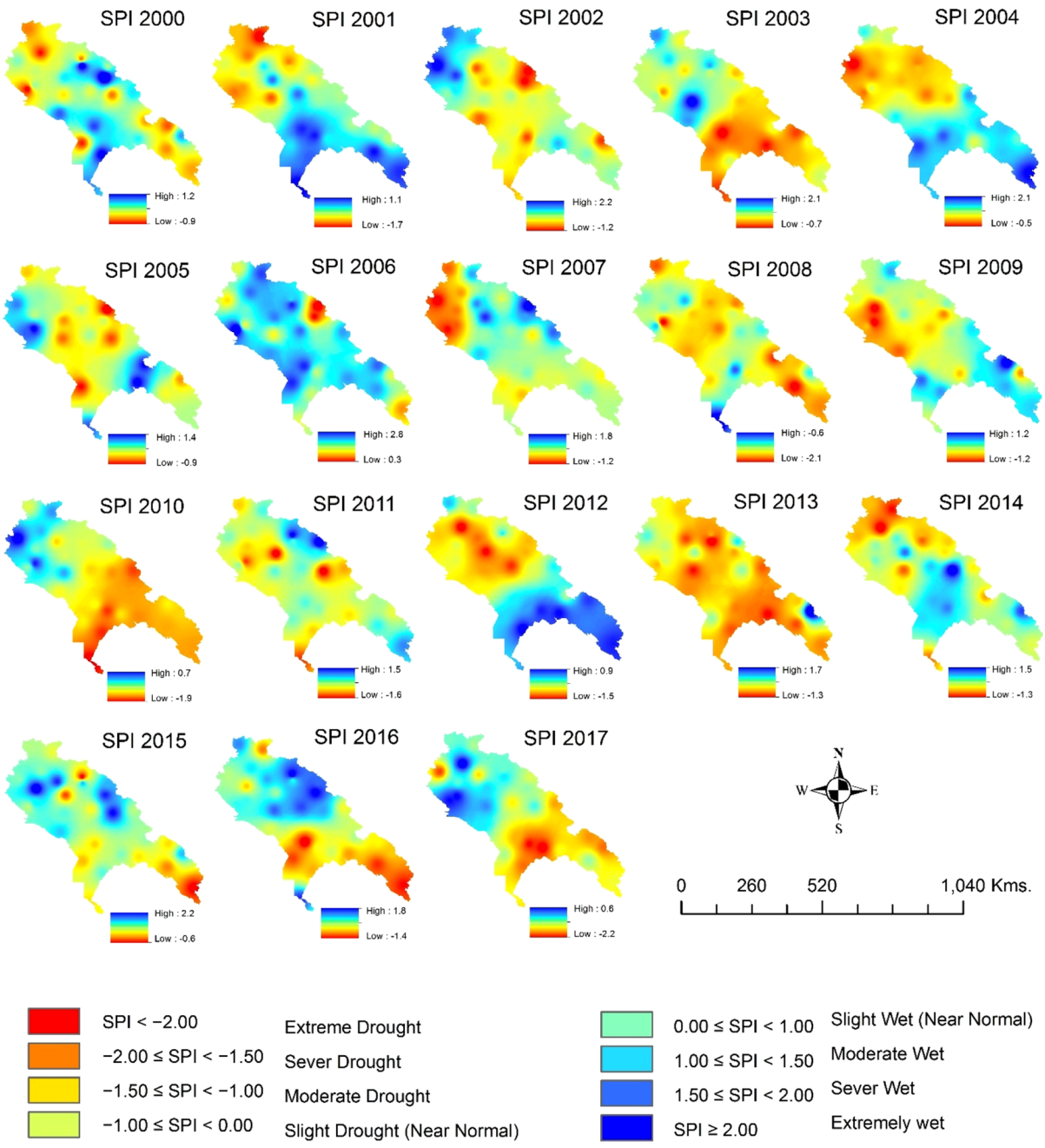

Fig. 5 Annual SPI for the study area during 2000–2017

In the study period, the years 2008 and 2017 were the driest years with − 1.56 and − 0.94 SPI index, respectively, and the years 2004 and 2006 were the wettest years with SPI indices 0.84 and 1.66, respectively. The mean coverage of all of NDVI categories in the study period and in the winter season was 5145 km^2. Figure 7 shows the relationship between the winter season NDVI and SPI. As it can be seen, in the time series (2000–2017), with regard to SPI index, we can divide the study period to two periods as wet period (2000–2007) and dry period (2008–2017)

Table 4 Vegetation coverage (km^2) and SPI in whole study area (2000–2017)

Year	Yearly SPI	Vegetation coverage (km^2)
2000	− 1/32 moderately drought	14,870
2001	0/71 slight wet (near normal)	19,364
2002	0/45 slight wet (near normal)	21,574
2003	0/51 slight wet (near normal)	19,923
2004	2/19 extremely wet	22,591
2005	0/28 slight wet (near normal)	19,110
2006	1/61 very wet	21,629
2007	0/89 slight wet (Near normal)	22,085
2008	− 2/2 extreme drought	14,713
2009	1/23 moderately wet	21,644
2010	− 0/91 slight wet (near normal)	25,198
2011	− 0/70 slight drought (near normal)	18,897
2012	0/25 slight wet (near normal)	19,367
2013	− 1/01 moderately drought	24,502
2014	1/27 moderately wet	25,416
2015	2/2 extremely wet	25,770
2016	0/52 slight wet (near normal)	26,578
2017	− 0/23 slight drought (near normal)	22,036
Average	0.31 slight wet (near normal)	Historical average 21,404

Table 5 The areas under each of the NDVI classes (km^2) in whole study area (2000–2017)

YEAR	NDVI 0.2–0.3	NDVI 0.3–0.4	NDVI 0.4–0.5	NDVI 0.5–0.6	NDVI 0.6–0.7	NDVI 0.7–0.8
2000	11,649	2342	580	205	74	21
2001	14,008	3900	1032	313	99	13
2002	15,012	4479	1338	533	183	29
2003	14,046	4298	1093	367	107	12
2004	15,425	4946	1503	522	168	27
2005	13,554	4020	1108	339	84	5
2006	14,878	4719	1394	477	151	11
2007	14,274	5434	1790	490	92	5
2008	11,597	2275	592	205	42	3
2009	14,893	4876	1389	406	77	3
2010	14,997	6487	2628	890	188	9
2011	13,425	3876	1127	362	100	6
2012	14,607	3704	770	226	57	3
2013	16,389	5747	1653	518	177	19
2014	16,768	6412	1644	457	125	9
2015	16,741	6439	1871	553	154	11
2016	15,656	7248	2621	815	213	24
2017	14,796	5094	1491	467	172	16
Average	11,649	2342	580	205	74	21

Table 6 The correlation between yearly SPI with yearly spatial coverage of NDVI in period of 2000–2017 with confidence level 95% (significant (*))

	NDVI 0.2–0.3	NDVI 0.3–0.4	NDVI 0.4–0.5	NDVI 0.5–0.6	NDVI 0.6–0.7	NDVI 0.7–0.8
Correlation	0/50 *	0/34	0/19	0/15	0/19	0/12
p value	0/04	0/16	0/46	0/55	0/46	0/64

Table 7 The correlation between seasonal SPI with seasonal spatial coverage of NDVI in period of 2000–2017 with confidence level 95%

SEASON	NDVI 0.2–0.3	NDVI 0.3–0.4	NDVI 0.4–0.5	NDVI 0.5–0.6	NDVI 0.6–0.7	NDVI 0.7–0.8
Winter	0.09	−0.05	−0.05	0.04	0.15	0.37
Spring	−0.10	0.77*	0.71*	0.63*	0.56*	0.41
Summer	0.12	0.11	0.09	0.01	−0.17	−0.13
Fall	0.70*	0.43	0.27	0.22	0.12	0.01

* Denotes significant at $p = 0.05$

(Fig. 7). As shown in Fig. 7, we cannot do the division for NDVI, too. In this season, the years of 2008 and 2017 had the driest winter with SPI index − 1.53 and − 1.39, respectively. The spatial coverage of all types of NDVI has got negative anomalies. This drought had the strongest effect on the NDVI of 0.2–0.6 than other categories (Table 9). Also in this season, the years of 2004 and 2006 had the driest winter with SPI index − 1.27 and − 2.14, respectively. The spatial coverage of all types of NDVI had a positive anomaly in the year of 2004. In spite of having the wettest winter in the study period in the year of 2006, because of very low temperature and freezing temperature in 12 stations during the winter season, especially in December (Aligodarz (− 3.9), Brojen (− 6.1), Broojerd (− 1.5), Kangavar (− 1.2), Kouhrang (− 7.8), Malayer (− 1.4), Dorood (0.0), Marivan (0.0), Norabadelorestan (− 2.3), Sanandaj (− 0.2), Shahrekord (− 6.5) and Yasouj (0.0), all types of the NDVI had a negative anomaly (Table 9), where the average temperature of the study area in the study period in December was 6.9 °C, and the average temperature of the month in the year 2006 fell to 2.8 °C; also in January and February the temperature (3.7 °C) was 1 °C lower than monthly average (4.7 °C) of the study period. Eventually because of this low temperature, all of the vegetation could not grow adequately in the winter season. Overall, Fig. 7 shows an increasing trend in the spatial coverage of NDVI range of 0.2–0.7 in the season in the study period.

Spring and winter seasons are special seasons in the study area because there is some of the great agricultural plain in the area, and that period is the growing and agricultural season. Figure 8 shows the relationship between the NDVI and SPI for spring season. The mean coverage of all of NDVI categories in the study period and in this season was 8936 km^2. In the time series (2000–2017), the years of 2000 and 2008 were the driest spring season with SPI index − 1.15 and − 1.85, respectively. Also, the spatial coverage of NDVI in those years had been 6374 km^2 and 6818 km^2, respectively, showing that they are among the least coverage years in the study period. The years of 2004 and 2015 had the wettest fall season (2.19 and 2.52 SPI index) that the spatial coverage of NDVI in those years had been 8853 km^2 and 9372 km^2, respectively, since they are among the highest coverage years in the study period. It has come from this reason that spring season is the growing season in the study area and also the temperature is relatively high (17.1 °C), and any changes in precipitation can directly affect the vegetation cover. So, there is a good correlation between almost NDVI categories with spring SPI, where the correlation between NDVI categories (0.3–0.7) is statistically significant and also the correlation between NDVI (0.7–0.8) is relatively high. There was a relatively higher agreement between the springtime NDVI categories and SPI than other seasons in the study period (Table 4 and Fig. 8). Overall, Fig. 8 shows an obvious increasing in the spatial coverage of NDVI categories (0.2–0.7) in the season in the study period.

Figure 9 shows the relationship between the summertime NDVI and SPI. The mean coverage of all of NDVI categories in the study period and in this season was 3719 km^2. In the time series (2000–2017), the years of 2006 and 2011 had the driest summer season with SPI index − 1.41 and − 1.12, respectively. Also, the spatial coverage of NDVI in

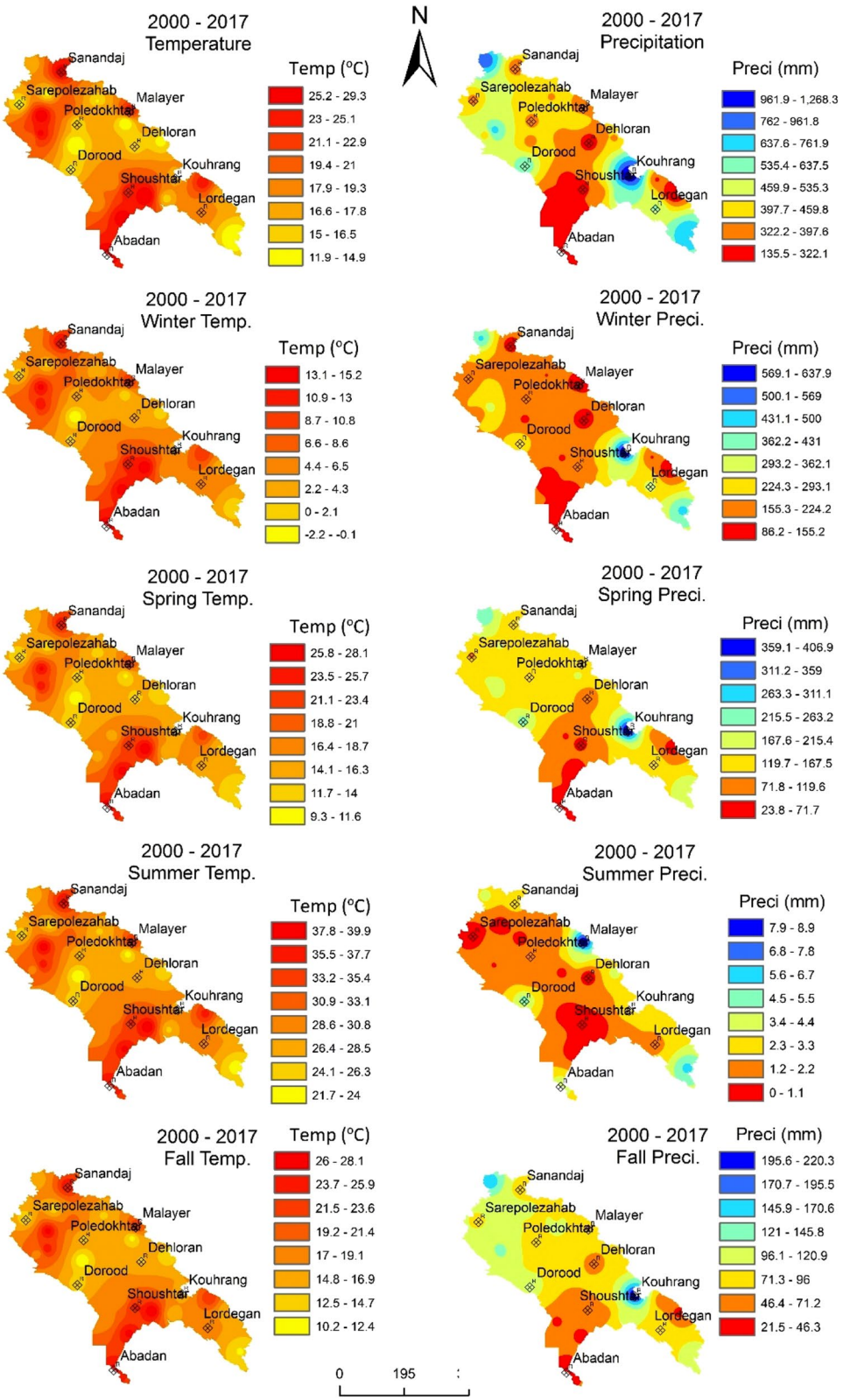

Fig. 6 Annual and seasonal average of precipitation and temperature of the study area in 2000–2017

Table 8 Descriptive information of seasonal precipitation and temperature of the study area (2000–2017)

Precipitation (mm)	Average in the whole study area	Max in the whole study area	Station name (max occurred)	Min in the whole study area	Station name (min occurred)
Winter	213/6	638	Kouhrang	86/2	Abadan
Spring	139/1	407	Kouhrang	23/8	Abadan
Summer	2/2	8/9	Malayer	0/0	Shoushtar
Fall	88/3	220/4	Kouhrang	21/5	Abadan
Temperature (°C)	Average in the whole study area	Max in the whole study area	Station name (Max occurred)	Min in the whole study area	Station name (Min occurred)
Winter	6/2	15/2	Shoushtar	− 2/3	Kouhrang
Spring	17/1	28/1	Shoushtar	9/3	Kouhrang
Summer	30/0	40	Shoushtar	21/7	Kouhrang
Fall	19/1	29/3	Shoushtar	11/9	Kouhrang

those years was 3712 km^2 and 3618 km^2, respectively. The years of 2001 and 2015 have been the wettest summer seasons (1.02 and 2.74 SPI index); also the spatial coverage of NDVI in those years had been 3733 km^2 and 3931 km^2, respectively. It seems that is because of lacking precipitation in this season in the study area, when there is some water, the vegetation can grow up and it can affect the NDVI coverage of this year. When the precipitation is well distributed in all parts of the study area, the effects can be considerable and otherwise the changes cannot be remarkable. For example, precipitation in the year of 2001 has been distributed in 50% of the stations (15 stations), and in the year of 2015 it has been distributed in 90% of the stations (27 stations), so the coverage of vegetation was higher in 2015 than 2001. There is an agreement between SPI with summer season NDVI categories coverage, but it is not statistically significant (Tables 4, 5 and Fig. 9). Overall, this figure shows an increasing trend in the spatial coverage of NDVI range of 0.2–0.7 in the season in the study period.

Figure 10 shows the relationship between the NDVI and SPI for fall season. The mean coverage of all of NDVI categories in the study period and in this season was 3607 km^2. In the time series (2000–2017), the years of 2007 and 2016 had the driest summer season with SPI index − 1.34 and − 1.48, respectively. Also, the spatial coverage of NDVI in those years was 3169 km^2 and 3406 km^2, respectively. The years of 2009 and 2015 had the wettest summer season (1.43 and 1.95 SPI index); also the spatial coverage of NDVI in those years was 4533 km^2 and 4078 km^2, respectively. As it showed, year 2015 was the wettest year in the study period, so the high positive anomaly of precipitation can lead to an increase in the water levels in dams as well as raise the underground water and fill the aquifers. Therefore, the above-mentioned water supplies helped the vegetation cover to be high in the next year (2016) in spite of a moderate drought. The opposite was true for the year 2009 because of severe drought in the year 2008 (Table 4 and Fig. 10). There is harmony between SPI with fall season NDVI categories coverage, that it is statistically significant for NDVI 0.2–0.3; and also it is relatively high for NDVI 0.3–0.4 ($r = 0.43$, $p = 0.06$); and for the other NDVI categories, it is not considerable (Tables 4, 5 and Fig. 10). Overall, this figure showed an increasing trend in the spatial coverage of NDVI categories between 0.2 and 0.7 in the season in the study period.

Conclusion

In this study, the annual and seasonal drought-prone areas in the western and southwestern watersheds in Iran were identified using remote sensing, time-series analysis and geo-spatial technology. The drought risk areas were delineated by integrating satellite images and meteorological information data (using SPI as a proxy for drought). Therefore, our findings can partly fill the knowledge gap of these watersheds in Iran due to the absence of in situ measured data. We argue that given the enough datasets collected from point-based in situ measurement and satellite-borne platforms, a better

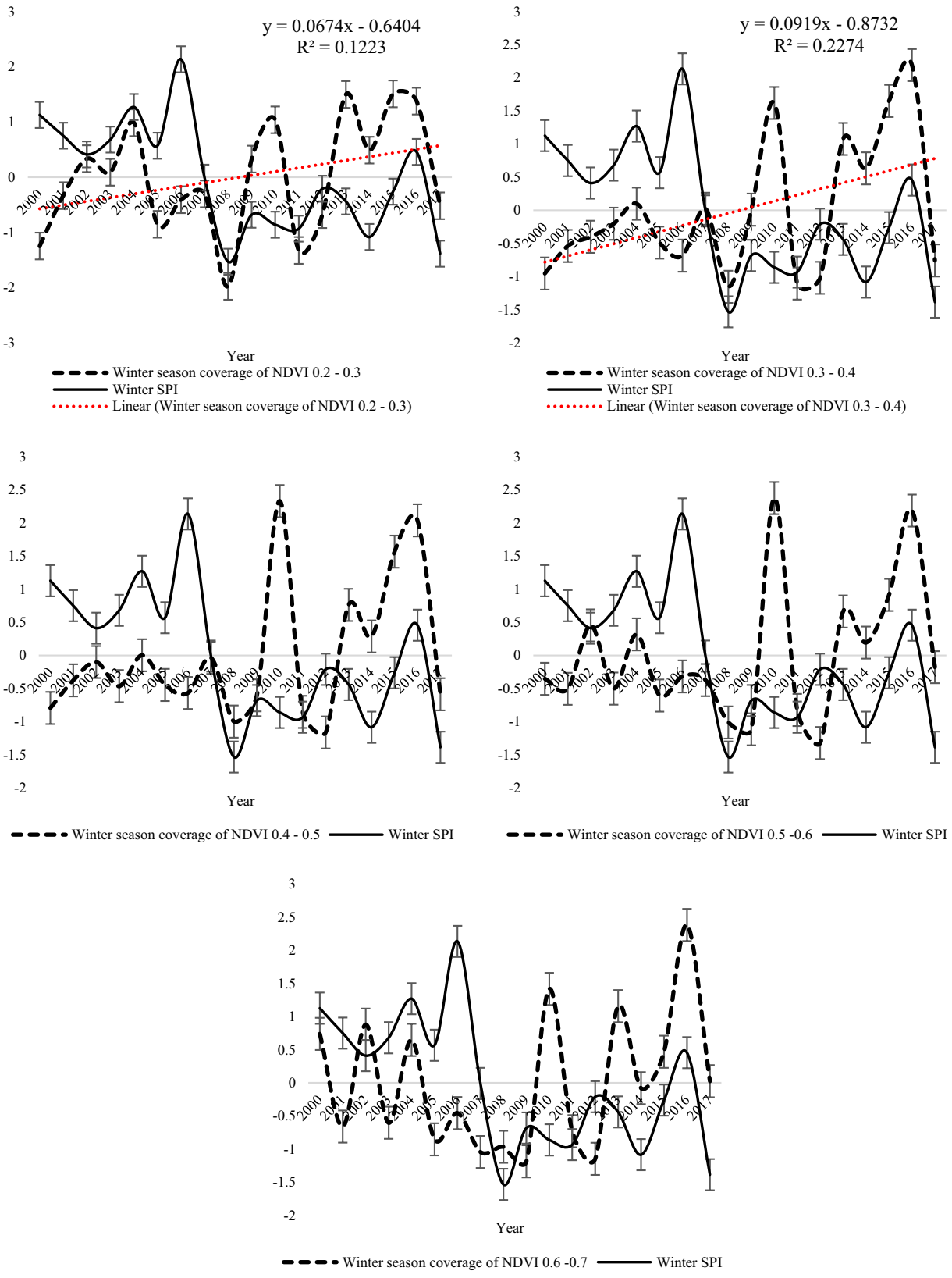

Fig. 7 Time series of winter season's NDVI and SPI for the whole study area (2000–2017)

Table 9 The anomaly of different NDVI categories in the winter's wettest (W) and driest (D) years in the study period (2000–2017)

	2008 (dry)	2017 (D)	2004 (wet)	2006 (W)
NDVI 0.2–0.3	− 1/98	− 0/52	0/99	− 0/41
NDVI 0.3–0.4	− 1/15	− 0/76	0/10	− 0/68
NDVI 0.4–0.5	− 1/00	− 0/59	0/00	− 0/57
NDVI 0.5–0.6	− 1/01	− 0/18	0/32	− 0/32
NDVI 0.6–0.7	− 0/97	0/03	0/65	− 0/46
NDVI 0.7–0.8	− 0/79	− 0/23	1/21	− 0/42
NDVI 0.8–0.9	− 0/44	− 0/33	0/62	− 0/42

understanding of the cause–effect relationship between the drought and vegetation will be achieved. Based on findings, it was concluded that the NDVI anomaly's temporal variations are not strongly linked with SPI and there was almost no strong linear relationship between NDVI and SPI in annual and seasonal time scale. The dominant NDVI class in the study area ranges between 0.2 and 0.3, representing approximately 68% of the total vegetation coverage. There is just a statistically significant correlation between NDVI (0.2–0.3) with yearly SPI ($R^2 = 0.50$, $p = 0.04$). This seemed attributable to that most of the vegetation of the study area is shrubs and grasslands and that this kind of vegetation has had a high sensitivity to some seasonal SPI index. Vegetation in the study area was minimum in the summer season (3720 km^2) and maximum in the spring season (8936 km^2), that is somewhat consistent with Montazeri and Kefayat Motlagh (2018) discoveries. In the study area, winter season is the rainiest and coldest season, spring is semi-rainy with moderate temperature, summer is the driest and hottest season and fall is semi-rainy with cold temperature. The lowest temperature in all seasons of the study period occurred in Kouhrang station in the southeast of study area, as well as three of the wettest seasons were observed in this station. The wettest station in the summer season in the study area was Malayer station with average of 8.9 mm precipitation (East margin of study area). Spring SPI was significantly correlated with spatial coverage of spring NDVI (0.3–0.7) ($p < 0.05$). Correlation between SPI and spatial coverage of NDVI in the spring and fall seasons was higher than other seasons. Spring season is growing season in the study area, and also the temperature is relatively high (17.1 °C); and any changes in precipitation can directly affect the vegetation cover. Therefore, there is a good correlation between almost NDVI categories with spring SPI, where the correlation between NDVI (0.3–0.7) is statistically significant. There was a relatively higher agreement between the springtime NDVI categories and SPI than other seasons in the study period. Overall, Fig. 7 shows an increase in the spatial coverage of NDVI (0.2–0.7) in the season in the study period.

Temperature can have an important role in the relationship between SPI and NDVI, in particular when the temperature was at water freezing or lower levels, which hindered vegetation growth. Consequently, high values of SPI cannot lead to high coverage of vegetation, especially in winter season. In the study period, an increasing trend in the spatial coverage of NDVI range of 0.2–0.7 in winter season was observed in the study area. The vegetation coverage in one year can be affected by SPI index of the previous year. As when there is a very wet year, filling the dams and groundwater aquifers can help the growth of the vegetation in the next year. In such cases, in spite of having a moderate or severe drought in the year, there will be a high vegetation cover in the study area. Summer season is the driest season in the study area, when there is some water, the vegetation can grow up and it can affect the NDVI coverage. When the precipitation was well distributed in all parts of the study area, the effect can be considerable and otherwise the changes cannot be remarkable. There was harmony between SPI with the summer season NDVI categories coverage, but it was not statistically significant. There was an increasing trend in the spatial coverage of NDVI range of 0.2–0.7 in summer season in the study period. There was harmony between SPI with fall season NDVI categories coverage; it was statistically significant for NDVI (0.2–0.3), and also it was relatively high for NDVI (0.3–0.4) ($r = 0.43$). There was an increasing trend in the spatial coverage of NDVI ranging between 0.2 and 0.7 in the fall season across the study period. Thus, it can be concluded that NDVI index and SPI share a strong correlation in warm seasons such as spring and summer, where water is a major limiting factor for vegetation growth.

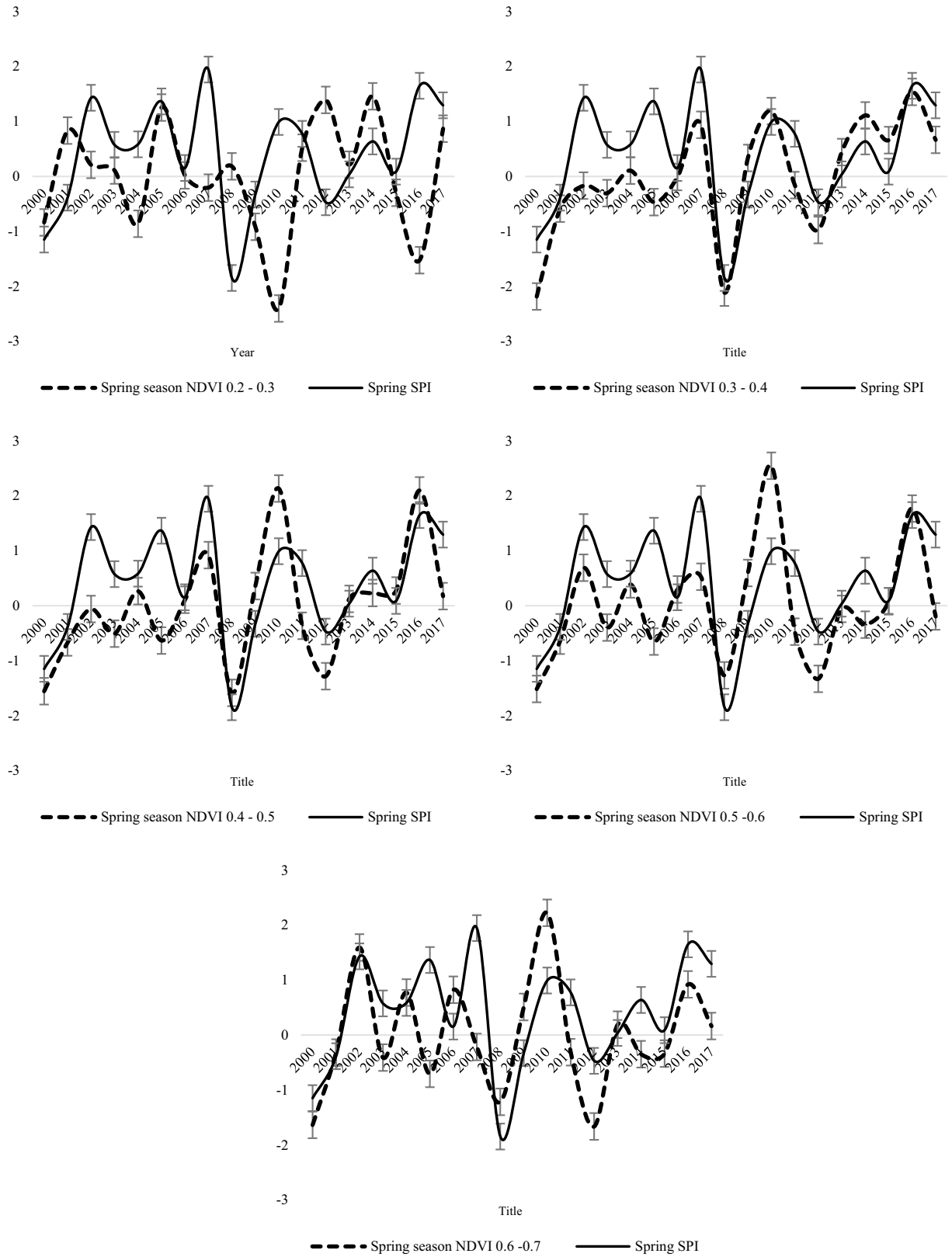

Fig. 8 Time series of spring season's NDVI and SPI for the whole study area (2000–2017)

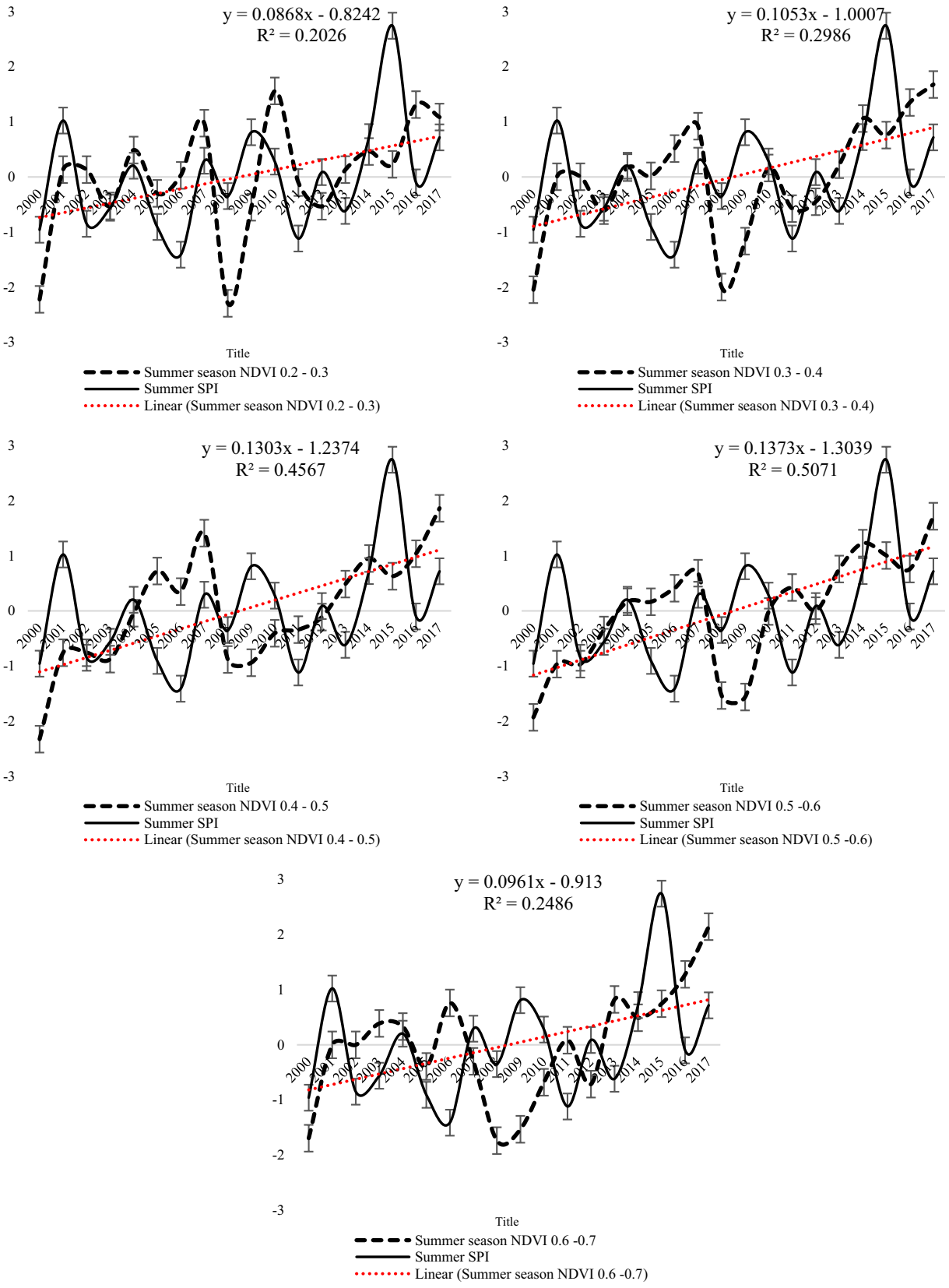

Fig. 9 Time series of summer season's NDVI and SPI for the whole study area (2000–2017)

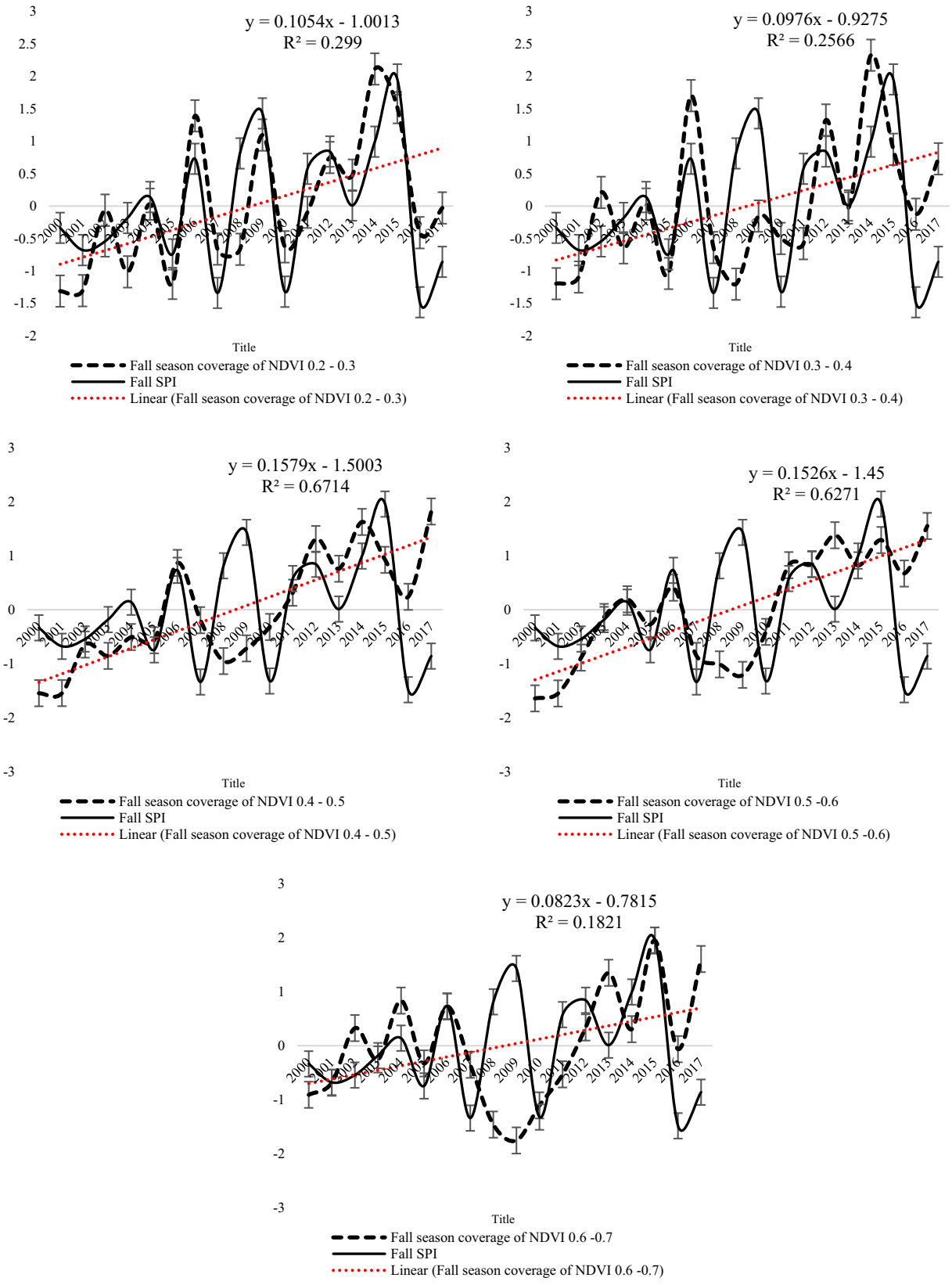

Fig. 10 Time series of fall season's NDVI and SPI for the whole study area (2000–2017)

Acknowledgements Iman Rousta is deeply grateful to his supervisor (Haraldur Olafsson, Professor of Atmospheric Sciences, Institute for Atmospheric Sciences-Weather and Climate, and Department of Physics, University of Iceland, and Icelandic Meteorological Office (IMO)) for his great support, kind guidance, and encouragement.

Author contributions IR and MdM proposed the topic. The corresponding authors, IR, and HZ, HO, MdM., JA, TDM, SS, and SA, commanded the data processing, analysis, and wrote the manuscript. IR, HO, MdM, JA, TDM, HZ, SS, and SA helped to enhance the research design, analysis, and manuscript writing.

Funding This work was supported by Vedurfelagid, Rannis and Rannsoknastofa i vedurfraedi.

Compliance with ethical standards

Conflict of interest The authors declare no conflict of interest.

Appendix

See Table 10.

Table 10 Studied meteorological stations

Station name	Geographical coordinate		Elevation (m)	Precipitation avg. (mm)	Temperature avg. (°C)
	X	*Y*			
Abadan	30/4	48/3	7	135/4	26/9
Ahwaz	31/3	48/7	23	186/4	27/2
Aligoodarz	33/4	49/7	2022	394/2	14/2
Bostan	32/0	51/3	2197	179/2	16/4
Brojen	31/7	48/0	8	249/8	18/2
Broojerd	33/9	48/8	1629	449/2	12/2
Dehloran	33/3	49/0	1522	244/4	15/1
Dorood	32/7	47/3	232	628/7	14/6
Eslamabadegharb	33/5	46/2	1171	436/2	19/8
Ilam	34/1	46/5	1349	522/8	28/0
Ivanegharb	33/6	46/4	1337	683/7	25/9
Izeh	31/9	49/9	767	575/3	15/7
Kangavar	33/3	47/4	1198	374/9	11/9
Kermanshah	34/5	48/0	1468	382/8	14/7
Khoramabad	34/4	47/2	1319	442/2	21/3
Kouhdasht	33/4	48/3	1148	382/5	16/9
Kouhrang	32/4	50/1	2285	1268/6	16/7
Lordegan	31/5	50/8	1580	541/9	18/1
Malayer	34/3	48/9	1778	330/5	24/9
Marivan	35/5	46/2	1287	854/9	16/9
Masjedsolayman	31/9	49/3	321	357/3	29/3
Norabadelorestan	34/3	48/0	1859	468/6	17/5
Poledokhtar	33/9	47/4	714	370/5	15/2
Ravansar	34/7	46/6	1380	482/4	14/5
Safiabad	32/3	48/4	83	279/2	18/0
Sanandaj	35/3	47/0	1373	346/5	26/8
Sarepolezahab	34/5	45/9	545	377/0	14/2
Shahrekord	32/3	50/9	2049	315/0	24/5
Shoushtar	32/1	48/8	67	279/5	24/9
Yasouj	30/8	51/7	1832	756/5	12/9

References

Bajgiran PR, Darvishsefat AA, Khalili A, Makhdoum MF (2008) Using AVHRR-based vegetation indices for drought monitoring in the Northwest of Iran. J Arid Environ 72:1086–1096

Bhuiyan C (2004) Various drought indices for monitoring drought condition in Aravalli terrain of India. In: XXth ISPRS congress, Istanbul, Turkey, pp 12–23

Bhuiyan C, Singh R, Kogan F (2006) Monitoring drought dynamics in the Aravalli region (India) using different indices based on ground and remote sensing data. Int J Appl Earth Obs Geoinf 8:289–302

Bordi I, Sutera A (2001) Fifty years of precipitation: some spatially remote teleconnnections. Water Resour Manag 15:247–280

Bordi I, Sutera A (2002) An analysis of drought in Italy in the last fifty years. Nuovo Cimento C Geophysics Space Phys C 25:185

Cancelliere A, Di Mauro G, Bonaccorso B, Rossi G (2007) Drought forecasting using the standardized precipitation index. Water Resour Manag 21:801–819

Chanklan R, Suksut K, Chaiyakhan K, Kaoungku N, Kerdprasop K, Kerdprasop N (2017) On applying regression and neural network to predict rainfall using satellite based index. In: Proceedings of the international multi conference of engineers and computer scientists, Hong Kong, China

Dabrowska-Zielinska K, Kogan F, Ciolkosz A, Gruszczynska M, Kowalik W (2002) Modelling of crop growth conditions and crop yield in Poland using AVHRR-based indices. Int J Remote Sens 23:1109–1123

Didan K (2015) MOD13Q1 MODIS/Terra vegetation indices 16-day L3 global 250 m SIN grid V006. NASA EOSDIS land processes DAAC

Dracup JA, Lee KS, Paulson EG Jr (1980) On the definition of droughts. Water Resour Res 16:297–302

Dutta D, Kundu A, Patel N, Saha S, Siddiqui A (2015) Assessment of agricultural drought in Rajasthan (India) using remote sensing derived Vegetation Condition Index (VCI) and Standardized Precipitation Index (SPI). Egypt J Remote Sens Space Sci 18:53–63

Fernandez-Raga M, Castro A, Marcos E, Palencia C, Fraile R (2017) Weather types and rainfall microstructure in Leon, Spain. Int J Climatol 37:1834–1842

Gandhi GM, Parthiban S, Thummalu N, Christy A (2015) NDVI: vegetation change detection using remote sensing and GIS—a case study of Vellore District. Proc Comput Sci 57:1199–1210

Geerken R, Zaitchik B, Evans J (2005) Classifying rangeland vegetation type and coverage from NDVI time series using Fourier Filtered Cycle Similarity. Int J Remote Sens 26:5535–5554

Ghafarian Malamiri H, Rousta I, Olafsson H, Zare H, Zhang H (2018) Gap-filling of MODIS time series land surface temperature (LST) products using singular spectrum analysis (SSA). Atmosphere 9:334

Gibbs WJ, Maher JV (1967) Rainfall deciles as drought indicators. In: Bulletin, vol 48. Commonwealth Bureau of Meteorology, Australia

Gitelson AA, Viña A, Arkebauer TJ, Rundquist DC, Keydan G, Leavitt B (2003) Remote estimation of leaf area index and green leaf biomass in maize canopies. Geophys Res Lett 30:1248

Goddard S, Harms SK, Reichenbach SE, Tadesse T, Waltman WJ (2003) Geospatial decision support for drought risk management. Commun ACM 46:35–37

Guttman NB (1998) Comparing the palmer drought index and the standardized precipitation index1. JAWRA J Am Water Resour Assoc 34:113–121

Ji L, Peters AJ (2003) Assessing vegetation response to drought in the northern Great Plains using vegetation and drought indices. Remote Sens Environ 87:85–98

Khosravi H, Haydari E, Shekoohizadegan S, Zareie S (2017) Assessment the effect of drought on vegetation in desert area using landsat data. Egypt J Remote Sens Space Sci 20:S3–S12

Kogan F (1990) Remote sensing of weather impacts on vegetation in non-homogeneous areas. Int J Remote Sens 11:1405–1419

Kogan F (2002) World droughts in the new millennium from AVHRR-based vegetation health indices. Eos Trans Am Geophys Union 83:557–563

Montazeri M, Kefayat Motlagh OR (2018) Long term mean of vegetation analysis in Iran using NDVI index. J Geogra Environ Plann 29:1–14

Martínez B, Gilabert MA (2009) Vegetation dynamics from NDVI time series analysis using the wavelet transform. Remote Sens Environ 113:1823–1842

McKee TB, Doesken NJ, Kleist J (1993) The relationship of drought frequency and duration to time scales. In: Proceedings of the 8th conference on applied climatology. American Meteorological Society, Boston, MA, pp 179–183

Moulin S, Kergoat L, Viovy N, Dedieu G (1997) Global-scale assessment of vegetation phenology using NOAA/AVHRR satellite measurements. J Clim 10:1154–1170

Mushore TD, Dube T, Manjowe M, Gumindoga W, Chemura A, Rousta I, Odindi J, Mutanga O (2019) Remotely sensed retrieval of local climate zones and their linkages to land surface temperature in Harare metropolitan city, Zimbabwe. Urban Clim 27:259–271

Palmer WC (1965) Meteorological drought. Research paper no 45. U.S. Department of Commerce Weather Bureau, Washington, DC

Palmer WC (1968) Keeping track of crop moisture conditions, nationwide: the new crop moisture index. pp 156–161

Rahimzadeh-Bajgiran P, Omasa K, Shimizu Y (2012) Comparative evaluation of the Vegetation Dryness Index (VDI), the Temperature Vegetation Dryness Index (TVDI) and the improved TVDI (iTVDI) for water stress detection in semi-arid regions of Iran. ISPRS J Photogramm Remote Sens 68:1–12

Rousta I, Khosh Akhlagh F, Soltani M, Modir Taheri Sh S (2014) Assessment of blocking effects on rainfall in northwestern Iran. In: COMECAP 2014. COMECAP, Heraklion, Grecce, pp 127–132

Rousta I, Doostkamian M, Haghighi E, Malamiri HRG, Yarahmadi P (2017a) Analysis of spatial autocorrelation patterns of heavy and super-heavy rainfall in Iran. Adv Atmos Sci 34:1069–1081

Rousta I, Doostkamian M, Taherian AM, Haghighi E, Ghafarian Malamiri HR, Ólafsson H (2017b) Investigation of the spatio-temporal variations in atmosphere thickness pattern of Iran and the Middle East with special focus on precipitation in Iran. Climate 5:82

Rousta I, Nasserzadeh MH, Jalali M, Haghighi E, Ólafsson H, Ashrafi S, Doostkamian M, Ghasemi A (2017c) Decadal spatial-temporal variations in the spatial pattern of anomalies of extreme precipitation thresholds (case study: Northwest Iran). Atmosphere 8:135

Rousta I, Javadizadeh F, Dargahian F, Olafsson H, Shiri-Karimvandi A, Vahedinejad SH, Doostkamian M, Monroy Vargas ER, Asadolahi A (2018a) Investigation of vorticity during prevalent winter precipitation in Iran. Adv Meteorol. https://doi.org/10.1155/2018/6941501

Rousta I, Sarif M, Gupta R, Olafsson H, Ranagalage M, Murayama Y, Zhang H, Mushore T (2018b) Spatiotemporal analysis of land use/land cover and its effects on surface urban heat island using

Landsat data: a case study of Metropolitan City Tehran (1988–2018). Sustainability 10:4433

Rousta I, Karampour M, Doostkamian M, Olafsson H, Zhang H, Mushore TD, Karimvandi AS, Vargas ERM (2020) Synoptic-dynamic analysis of extreme precipitation in Karoun River Basin, Iran. Arab J Geosci 13:1–16

Running SW, Loveland TR, Pierce LL, Nemani RR, Hunt ER Jr (1995) A remote sensing based vegetation classification logic for global land cover analysis. Remote Sens Environ 51:39–48

Shafer B (1982) Developemnet of a surface water supply index (SWSI) to assess the severity of drought conditions in snowpack runoff areas. In: Proceedings of the 50th annual western snow conference, Colorado State University, Fort Collins

Shah R, Bharadiya N, Manekar V (2015) Drought index computation using standardized precipitation index (SPI) method for Surat District, Gujarat. Aquat Proc 4:1243–1249

Smitha P, Narasimhan B, Sudheer K, Annamalai H (2018) An improved bias correction method of daily rainfall data using a sliding window technique for climate change impact assessment. J Hydrol 556:100–118

Tarpley J, Schneider S, Money R (1984) Global vegetation indices from the NOAA-7 meteorological satellite. J Clim Appl Meteorol 23:491–494

Thenkabail PS, Gamage MSDN (2004) The use of remote sensing data for drought assessment and monitoring in Southwest Asia, vol 85. Iwmi

Thom H (1966a) Some methods of climatological analysis, WMO technical note. Number 81, Secretariat of the World Meteorological Organization, Geneva, Switzerland

Thom H (1966b) Some methods of climatological analysis. WMO Tech. Note 81

Townshend JR, Justice C (1986) Analysis of the dynamics of African vegetation using the normalized difference vegetation index. Int J Remote Sens 7:1435–1445

Yu X, Xin P, Lu C, Robinson C, Li L, Barry DA (2017) Effects of episodic rainfall on a subterranean estuary. Water Resour Res 53:5774–5787